

Published in final edited form as:

Nat Methods. 2019 November ; 16(11): 1105–1108. doi:10.1038/s41592-019-0554-0.

The mesoSPIM initiative – open-source light-sheet microscopes for imaging cleared tissue

Fabian F. Voigt^{1,2}, Daniel Kirschenbaum³, Evgenia Platonova⁴, Stéphane Pagès^{5,6}, Robert A. A. Campbell⁷, Rahel Kastli^{1,2}, Martina Schaettin^{8,2}, Ladan Eglolf^{1,2}, Alexander van der Bourg^{1,2}, Philipp Bethge^{1,2}, Karen Haenraets^{9,2}, Noémie Frézel^{9,2}, Thomas Topilko¹⁰, Paola Perin¹¹, Daniel Hillier^{12,13}, Sven Hildebrand¹⁵, Anna Schueth¹⁵, Alard Roebroek¹⁵, Botond Roska^{16,17}, Esther T. Stoeckli^{8,2}, Roberto Pizzala¹⁸, Nicolas Renier⁹, Hanns Ulrich Zeilhofer^{9,2}, Theofanis Karayannis^{1,2}, Urs Ziegler⁴, Laura Batti⁵, Anthony Holtmaat⁶, Christian Lüscher^{6,19}, Adriano Aguzzi³, Fritjof Helmchen^{1,2}

¹Brain Research Institute, University of Zurich

²Neuroscience Center Zurich, University of Zurich and ETH Zurich

³University Hospital Zurich

⁴Center for Microscopy and Image Analysis, University of Zurich

⁵Wyss Center for Bio- and Neuroengineering, Geneva

⁶Department of Basic Neurosciences, University of Geneva

⁷Sainsbury Wellcome Centre for Neural Circuits and Behaviour, London

⁸Institute of Molecular Life Sciences, University of Zurich

⁹Institute of Pharmacology and Toxicology, University of Zurich

¹⁰ICM - Brain & Spine Institute, Paris

¹¹Department of Brain and Behavioural Sciences, University of Pavia

Users may view, print, copy, and download text and data-mine the content in such documents, for the purposes of academic research, subject always to the full Conditions of use:http://www.nature.com/authors/editorial_policies/license.html#terms

Corresponding author: Correspondence to Fabian Voigt. voigt@hifo.uzh.ch.

Code availability

The mesoSPIM software and documentation are available as Supplementary Software. Updated versions can be found on Github (<https://github.com/mesoSPIM>). mesoSPIM-control is licensed under the GNU General Public License v3.0 (GPL v3).

Data availability

Data was deposited to the Image Data Resource (<http://idr.openmicroscopy.org>) under accession number IDR0066.

Author information – Contributions

F.F.V. and F.H. designed the project. F.F.V. designed the microscope, wrote control software and documentation, coordinated the mesoSPIM initiative, and analyzed data. F.F.V., E.P., and P.B. imaged samples. D.K., E.P., R.K., M.S., L.E., A. v.d. B., K. H., N.F., T.T., N.R., H-U. Z., T.K., P.P., R.P., D.H., B.R., S.H., A.S., A.R. prepared samples for imaging. F.F.V., S.P., E. P., D.K., R.A.A.C., F.M., U.Z., L.B. A.H., C.L., A.A. set up mesoSPIM instruments. F.F.V. and F.H. wrote the manuscript with input from all coauthors.

Competing interests

None to disclose.

Peer review information

Rita Strack was the primary editor on this article and managed its editorial process and peer review in collaboration with the rest of the editorial team.

¹²Hungarian Academy of Sciences Research Centre for Natural Sciences

¹³Faculty of Information Technology and Bionics, Pazmany Peter Catholic University

¹⁵Faculty of Psychology & Neuroscience, Maastricht University

¹⁶Friedrich Miescher Institute Basel

¹⁷Institute of Molecular and Clinical Ophthalmology Basel

¹⁸Department of Molecular Medicine, University of Pavia

¹⁹Clinic of Neurology, Dept. of Clinical Neurosciences, Geneva University Hospital

Abstract

Light-sheet microscopy is an ideal technique for imaging large cleared samples; however, the community is still lacking instruments capable of producing volumetric images of centimeter-sized cleared samples with near-isotropic resolution within minutes. Here, we introduce the mesoscale selective plane-illumination microscopy (mesoSPIM) initiative, an open-hardware project for building and operating a light sheet microscope that addresses these challenges and is compatible with any type of cleared or expanded sample (www.mesospim.org).

Over the course of the past decade, tissue clearing methods have reached a high level of sophistication with a wide variety of approaches now available¹. Common clearing techniques fall into two categories: Approaches using organic solvents, for example the DISCO family of protocols^{2–5}, and methods using aqueous solutions such as CLARITY⁶ and CUBIC^{7, 8}. To image samples processed with these methods, a wide range of commercial light-sheet microscopes can be utilized (Supplementary Note 1). Nonetheless, many users still experience significant shortcomings when using existing instruments to image cleared samples: For example, the imaging chamber, sample holders, and sample stages of microscopes designed for time-lapse imaging in developing embryos are usually undersized for cm-sized cleared samples. Even if the setup was specifically designed with clearing in mind, accommodating large samples can be a significant challenge: Modern clearing techniques can render a whole mouse central nervous system (CNS) or even entire mice^{4, 5} transparent; yet, there are no instruments capable of imaging such samples without cutting. In addition, many instruments achieve optimal image quality only for a limited selection of immersion media, often restricted by the specifications of existing microscope objectives. As typical refractive indices in light-sheet microscopy range from 1.33 (for water) to 1.56 (for a mixture of benzyl alcohol and benzyl benzoate, BABB⁹), this limits several commercial microscopes to a narrow subset of clearing techniques (Supplementary Table 1).

To overcome these limitations, we set out to design a modular light-sheet microscope that combines a large imaging volume, excellent image quality over large fields-of-view (FOV) with simple and versatile sample handling (Fig. 1a, Supplementary Note 2, Supplementary Video 1). To allow multi-view acquisitions, we adopted an instrument layout similar to the original selective plane illumination microscope (SPIM)¹⁰ with a horizontal detection path and a vertical sample rotation axis (Supplementary Fig. 1 and 2). The instrument is equipped

with a zoom macroscope in the detection path which allows FOVs of 2-21 mm in combination with a sCMOS camera. This enables users to view large samples and then zoom in to reveal minute details such as individual axons (Fig. 1c-e). Therefore, we have termed the instrument the mesoscale selective plane-illumination microscope (mesoSPIM).

To streamline sample handling, we use magnetic quick-exchange mounts for the immersion cuvettes and sample holders. These mounts allow rapid switching between different immersion media and samples within less than a minute (Supplementary Video 2). Samples are usually mounted in a cuvette¹¹ or clamped in a 3D-printed holder (Fig. 1a, Supplementary Fig. 3).

The mesoSPIM light-sheet is generated by rapidly scanning a Gaussian beam in the vertical plane using a galvo scanner similar to a digital scanned light-sheet microscope (DSLIM)¹². This approach has several advantages when imaging large cleared samples: Firstly, it results in uniform image brightness as each part of the FOV is illuminated with the same intensity. Secondly, when changing the detection FOV using the detection zoom, the height of the light-sheet can be easily adapted by regulating the amplitude of the galvo waveform. Finally, DSLIM illumination reduces shadow artefacts¹³: In light-sheet microscopy, any sample feature that absorbs or refracts the excitation light casts a shadow across the FOV. The resulting images are full of stripes along the illumination direction which complicates image analysis and visualization. Because in DSLM each part of the sample is illuminated with a scanned cone of excitation light, the shadow zone behind absorbing objects can be shortened by increasing the opening angle of the cone (equivalent to increasing the excitation NA). In the mesoSPIM, we use an NA of 0.15 to achieve homogenous illumination with minimal shadow artifacts.

A Gaussian beam with increased excitation NA does, however, have a reduced Rayleigh range which leads to axially blurred images outside of the narrow waist region of the light-sheet (Fig. 1b). As we deemed uniform axial resolution to be absolutely necessary to achieve the highest possible data quality, we integrated axially scanned light-sheet microscopy (ASLM)¹⁴ in the mesoSPIM (Fig. 1b, see Supplementary Note 3, and Supplementary Videos 3-5). In our ASLM implementation, we shift the excitation beam waist through the sample using an electrically tuneable lens (ETL) and synchronize this motion with the rolling shutter of the sCMOS camera. Therefore, only the axially most confined region of the light-sheet contributes to image formation comparable to earlier approaches using mechanical translation of the sample¹⁵. In ASLM mode the mesoSPIM achieves an axial resolution of $5.57 \pm 0.03 \mu\text{m}$ (FWHM, $n = 2170$ beads, $nD=1.45$) across a 3.29-mm FOV and $6.52 \pm 0.07 \mu\text{m}$ (FWHM, $n = 322$ beads, $nD=1.45$) across a FOV of 13.29 mm (Supplementary Note 4, Supplementary Figure 4). These features enable us to image a whole mouse brain ($\approx 1 \text{ cm}^3$) with isotropic sampling ($6.5 \mu\text{m}$) within 7-8 minutes resulting in a relatively small dataset (12-16 GB).

The microscope software (mesoSPIM-control, Supplementary Software) is written in Python and allows users to specify sequences of z-stacks using a table-based acquisition manager (Supplementary Note 5, Supplementary Fig. 5, Supplementary Video 6). The software can also be used to acquire large-scale tiling acquisitions, for example to visualize fine neurites

in the developing nervous system of a 7-day old chicken embryo resulting in a 880 GB dataset (Figure 2, Supplementary Video 7). To achieve optimum optical sectioning in ASLM, the amplitude and offset of the ETL waveform need to be adapted when changing the excitation wavelength, zoom, or the immersion medium and can even depend on the local refractive properties of the sample. Therefore, mesoSPIM-control allows users to select configuration files with default ASLM settings for different immersion media and to manually optimize ASLM parameters (Supplementary Video 8).

With a travel range of $44 \times 44 \times 100$ mm, large samples such as a whole mouse CNS can be imaged in their entirety (Fig. 1c, Supplementary Video 9). After acquiring overview datasets, users can zoom in and record multidimensional data at higher resolution by mosaic acquisitions, for example revealing cellular distribution and long-range axonal projections of Purkinje cells in the mouse cerebellum (Fig. 1d-e, Supplementary Videos 10-12).

We tested the instrument in combination with all major clearing techniques (Supplementary Note 6) including active⁷ and passive¹¹ CLARITY (Fig 1b-e, Supplementary Fig. 6 and 7, Supplementary Video 13) and CUBIC-X⁹ (Supplementary Fig. 8). Among organic solvent methods, we tested iDISCO⁴ (Supplementary Fig. 9, Supplementary Video 14) and BABB² (Fig. 2, Supplementary Fig. 10). To demonstrate multi-view acquisitions with the mesoSPIM, we imaged a BABB-cleared chicken embryo from multiple directions (Supplementary Fig. 11) and fused the resulting datasets using BigStitcher¹⁶ (Supplementary Fig. 12). Given its flexible sample holders, the mesoSPIM is compatible with a wide range of sample types ranging from *Drosophila melanogaster* (Supplementary Fig. 13, Supplementary Video 15) to cleared human cortex processed using MASH¹⁷ (Supplementary Fig. 14, Supplementary Videos 16 and 17).

Inspired by the openSPIM¹⁸ and openSPIN¹⁹ projects, the mesoSPIM hardware documentation and software are freely available. Depending on the configuration, a mesoSPIM requires a budget of \$170000-\$240000 (Supplementary Table 2) and can be installed in a day if all parts are available (Supplementary Video 18). Currently, five mesoSPIM setups are in operation across Europe and several more instruments are under construction. The mesoSPIM is the ideal instrument to quickly bridge scales from the μm - to the cm-level which enables it to serve as an excellent tool for detailed three-dimensional anatomical investigations in neuroscience and developmental biology. We have designed the mesoSPIM as a versatile and modular imaging platform and expect that it will be extended towards even larger samples, combined with novel clearing methods, and integrated with other imaging modalities such as optical projection tomography²⁰.

Supplementary Material

Refer to Web version on PubMed Central for supplementary material.

Acknowledgements

This work was supported by grants from the Swiss National Science Foundation (grant nos. 31003A-149858, 31003B-170269 to F.H.; no. 31003A_170037 to T.K.; nos. 31003A-153448, 31003A_173125, CRSII3_154453 and NCCR Synapsy no. 51NF40-158776 to A.H.), the European Research Council (ERC Advanced Grant no. BRAINCOMPACT, project no. 670757 to F.H.), an ERC Starting Grants (InterWiring, project no. 679175 to T.K.

and MULTICONNECT, project no. 639938 to A.R.), the Dutch science foundation (NWO VIDI Grant, project no. 14637 to A.R.), a PhD fellowship by the Swiss Foundation for Excellence in Biomedical Research (to R.K), a gift from a private foundation with public interest through the International Foundation for Research in Paraplegia (to A.H. and S.P.), and a Distinguished Scientist Award of the Nomis Foundation (to A.A.). In addition, we would like to thank D. Göckeritz-Dujmovic and S. Bichet for help with sample preparation and M. Wieckhorst for help with custom electronics.

References

1. Richardson DS, Lichtman JW. *Cell*. 2015; 162:246–257. [PubMed: 26186186]
2. Ertürk A, et al. *Nature Protocols*. 2012; 7:1983–1995. [PubMed: 23060243]
3. Renier N, et al. *Cell*. 2014; 159:896–910. [PubMed: 25417164]
4. Pan C, et al. *Nat Methods*. 2016; 13:859–867. [PubMed: 27548807]
5. Cai R, et al. *Nat Neurosci*. 2019; 22:317–327. [PubMed: 30598527]
6. Chung K, et al. *Nature*. 2013; 497:332–337. [PubMed: 23575631]
7. Susaki EA, et al. *Cell*. 2014; 157:726–739. [PubMed: 24746791]
8. Murakami TC, et al. *Nature Neuroscience*. 2018; 1
9. Dodt H-U, et al. *Nature Methods*. 2007; 4:331–336. [PubMed: 17384643]
10. Huisken J, Swoger J, Del Bene F, Wittbrodt J, Stelzer EH. *Science*. 2004; 305:1007–1009. [PubMed: 15310904]
11. Tomer R, Ye L, Hsueh B, Deisseroth K. *Nat Protocols*. 2014; 9:1682–1697. [PubMed: 24945384]
12. Keller PJ, Schmidt AD, Wittbrodt J, Stelzer EHK. *Science*. 2008; 322:1065–1069. [PubMed: 18845710]
13. Fahrbach FO, Simon P, Rohrbach A. *Nat Photon*. 2010; 4:780–785.
14. Dean KM, Roudot P, Welf ES, Danuser G, Fiolka R. *Biophysical Journal*. 2015; 108:2807–2815. [PubMed: 26083920]
15. Buytaert JAN, Dirckx JJJ. *Journal of Biomedical Optics*. 2007; 12
16. Hörl D, et al. *Nat Methods*. 2019; 16:870–874. [PubMed: 31384047]
17. Hildebrand S, Schueth A, Herrler A, Galuske R, Roebroek A. *Sci Rep*. 2019; 9
18. Pitrone PG, et al. *Nat Methods*. 2013; 10:598–599. [PubMed: 23749304]
19. Gualda EJ, et al. *Nat Methods*. 2013; 10:599–600. [PubMed: 23749300]
20. Sharpe J, et al. *Science*. 2002; 296:541–545. [PubMed: 11964482]

Editor's summary

The mesoSPIM is an open hardware axially scanned light-sheet microscope for the rapid imaging of large cleared samples with isotropic resolution.

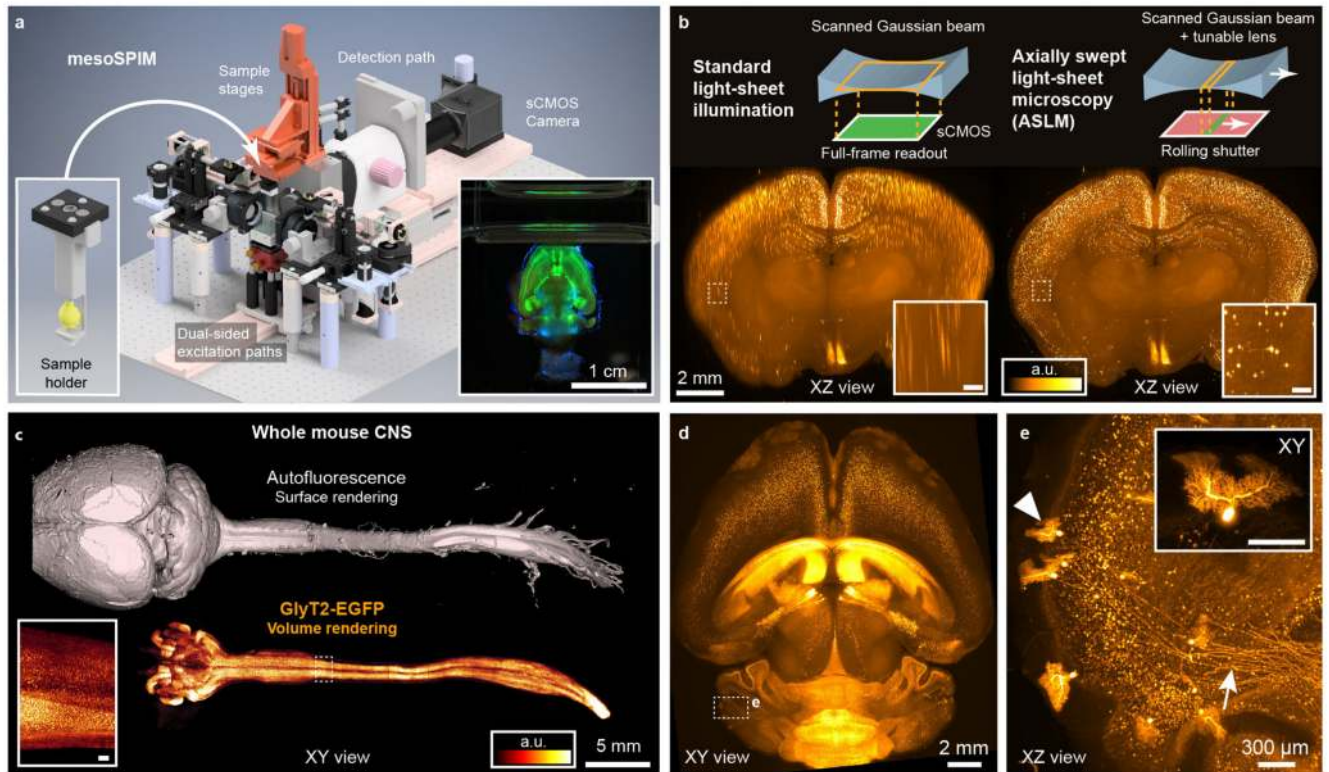


Figure 1. Example demonstrations of the mesoSPIM light-sheet mesoscope.

a) Overview of the mesoSPIM instrument (Version 4). Left inset: 3D-printed sample holder with magnetic quick-exchange mount. Alternatively, samples can be mounted in a cuvette. Right inset: Photograph of a Thy1-YFP mouse brain during image acquisition. **b)** Comparison of axial image quality achieved in a CLARITY-cleared VIP-tdTomato mouse brain for standard light-sheet illumination (left) and for the axially swept light-sheet mode, ASLM (right). Images are maximum intensity projections over 250- μ m range. **c)** Whole-CNS imaging with the mesoSPIM. A whole central nervous system was dissected from a Glycine Transporter-2 EGFP (GlyT2-EGFP) mouse and cleared using the X-CLARITY protocol. The inset shows glycinergic neurons in a subregion of the spinal cord. **d)** Overview image of a CLARITY-cleared TPH2Cre-tdTomato mouse brain. **e)** Volume rendering of sparsely labeled Purkinje cells and their axonal projections (arrow) from the dashed box in (d). Inset: individual Purkinje cell (arrow head). Panels (d) and (e) use the same colorbar as (b). Scale bars of all insets: 200 μ m. The imaging experiments were conducted once using animals aged 6 weeks (c) and 2 months (d).

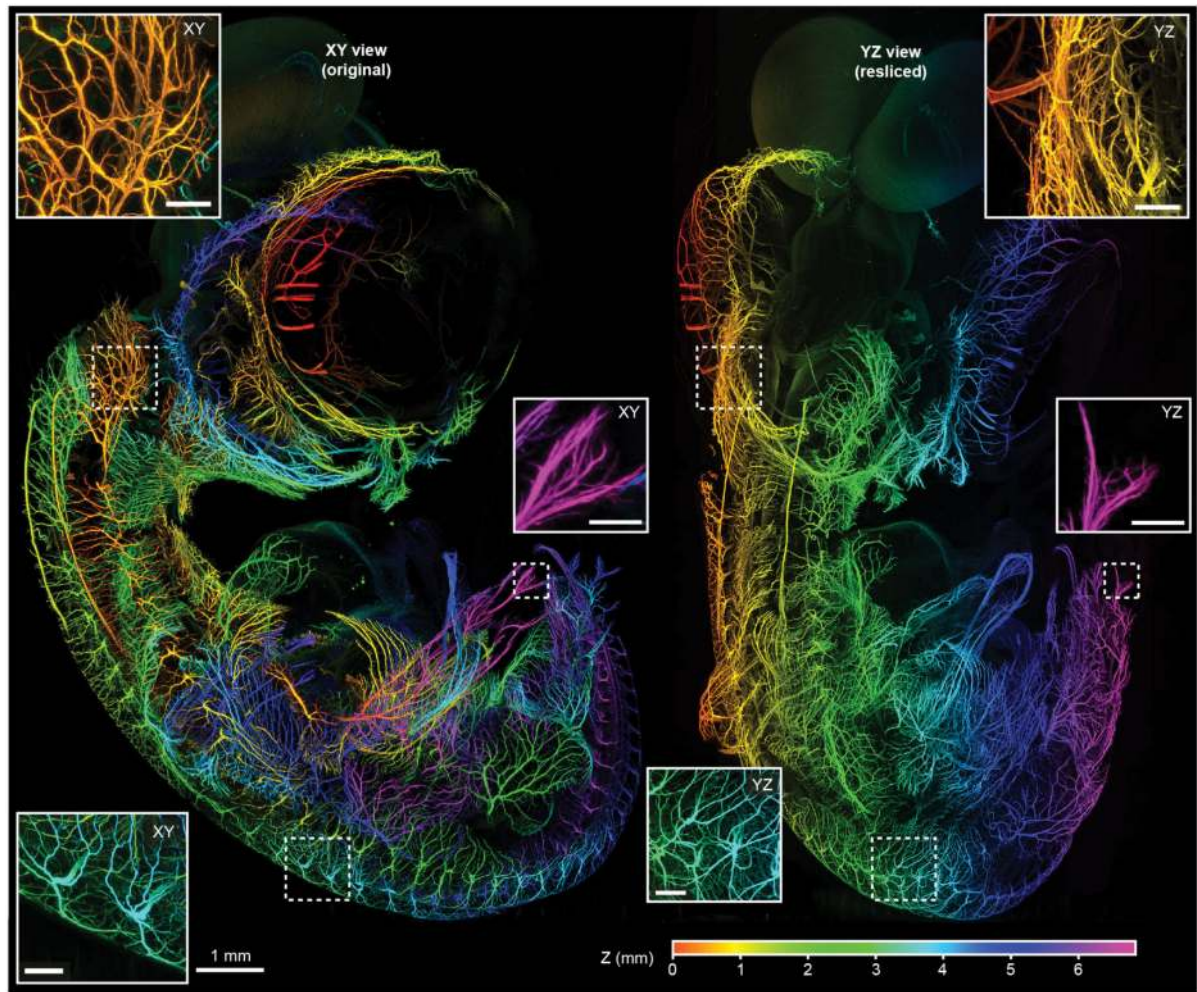


Figure 2. Large scale-dataset acquired with the mesoSPIM:

Depth-coded original XY (left) and resliced YZ (right) projections of a dataset taken from a 7-day old chicken embryo (neurofilament labeling) cleared using BABB. Throughout the dataset (acquired at $1.6 \times 1.6 \times 2 \mu\text{m}^3$ sampling), neurites are visible in great detail. Because of the ASLM mode the same holds true for the original (transverse) and the resliced (axial) direction. The assignment of color to Z-position is similar for both the XY and YZ view. Scale bars of all insets: $200 \mu\text{m}$. The imaging experiment was conducted once.